Journal of Materials Chemistry C

Accepted Manuscript

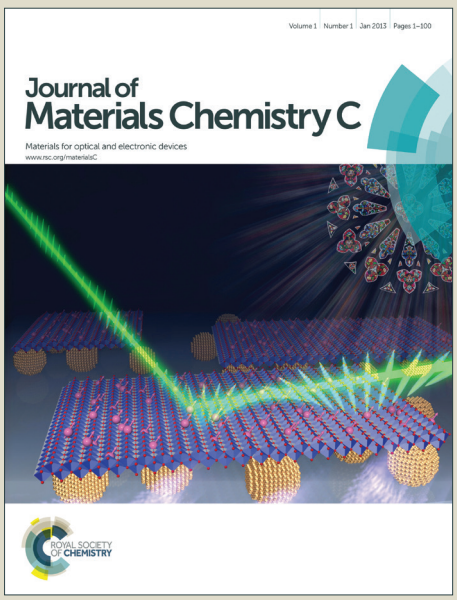

ROYAL SOCIETY OF CHEMISTRY

www.rsc.org/materialsC

Synthesis and characterization of conductive few layer graphene nanosheets by anionic electrochemical intercalation and exfoliation technique

Sumanta Kumar Sahoo* and Archana Mallik

Electrometallurgy and Corrosion Laboratory, Department of Metallurgical and Materials Engineering, National Institute of Technology Rourkela-769008, Odisha, India.

Abstract:

The mechanism of electrochemical intercalation resulting expansion and exfoliation behavior of the pyrolytic graphite sheets has been discussed. Presently, an efficient and simple process of the intercalation of perchlorate anions from a simple protic solvent at various electrolytic concentrations has been explored by a two electrode system. The intercalate concentration plays a major role in the as-prepared exfoliated few layered graphene nanosheets (FLGNSs). The in-situ oxygenation and hydroxylation of the FLGNSs has been elaborately analysed and discussed by X-ray diffraction, Thermogravimetric analysis, Fourier transform infrared spectroscopy, X-ray photoelectron spectroscopy, Raman spectroscopy and UV-visible spectroscopy. Furthermore, the nature of the exfoliated FLGNSs colloidal were analysed by Field emission scanning electron microscopy, Transmission electron microscopy as well as dynamic light scattering technique. From various analyses, it is found that the synthesized GNSs consists of few layered graphene nanosheets with surface oxygenation. The extent of surface oxygenation was found to be increased with rise in intercalate concentrations. The exfoliated graphene colloidal obtained at an optimum electrolytic condition shows stable dispersion and highest conductivity of ~ 0.87mS/cm. Further the conductivity of the oven dried the graphene colloidal on fluoride treated glass slide has been successfully tested by a light emitting diode fabrication test.

Keywords: Graphene nanosheets, Electrochemistry, Intercalation, Exfoliation, Colloids.

1. Introduction

Limitations in substrate transformation, environmental concerns, complicated and un-economical route to synthesize high quality GNSs has certainly instigated many researchers to explore the most versatile science of electrochemistry towards the synthesis as well as analyze the product. This top-down technique has several advantages, including simple instrumentation, cost-effectiveness, being green (no use of toxic chemicals), single step process and low temperature operation. This approach may use either a simple or specialized graphite substrate in simple ionic electrolytes at a suitable applied bias[1]. Depending upon negative (or positive) potential applied to the graphite substrate, the cationic (or anionic) intercalate from aqueous ionic electrolytes intercalate the stratified graphite and inhibit π-electrons bonding between the two layers[2].

* Corresponding author: Tel. : +91-661 2464555; Fax: +91- 661 2472926.
E-mail address: sumantakumarsahoo@live.com (S. K. Sahoo).

Furthermore, the simultaneous redox reactions lead to the evolution of gaseous species at the electrode surface and hence results in-situ stress generation. This synergistic phenomenon could also produce surface blistering of the graphite substrate. Consequently, single to few layer thin sheets of high quality graphene flake are dispersed in the electrolytic bath. Cations such as lithium ions, tetra-alkyl-ammonium ions, lithium-propylene carbonate ionic complexes and N-butyl-methylpyrrolidium ions[3–6] and anions such as sulfate ions, perchlorate ions, nitrate ions, polystyrene sulfonate ions[7–10] been explored generously. Anodic intercalation followed by exfoliation has been reported to be more efficient (than the cathodic ones) in producing graphene flakes due to the nature and volume of evolution of gas at the graphite. The gases evolved at the electrode are mainly oxygen and carbon dioxide, and hydrogen during anodic and cathodic interacalation respectively. It is believed that a vigorous amount of voluminous gas evolution might lead to better intercalation during anodic processes. Though the exfoliation is expected to be better, there are also equal chances that newly formed graphene sheets will have attached oxygen atoms/molecules as a functional group. However, oxygen functional group such as hydroxyl, epoxy and carboxylic groups in anodic exfoliated graphene nanosheets can be minimized by suitable selection of concentration of electrolytes and potentials. Conversely according to a recent study graphene/graphene oxide thus produced are usually defective than those produced via other contemporary methods. The relatively higher amount of defects thus introduced in the electrochemically synthesized FLGNs may find interesting properties and hence after effects[11].

In this paper, the authors report a simple, fast and cost-effective approach of electrochemical intercalation and exfoliation for commercial scale synthesis of few-layered graphene nanosheets (FLGNSs) from pyrolytic graphite sheet through anionic intercalation by perchloric anions. The work is a continuation and assessment to the previously reported investigation[12] on effectiveness of another extensively used anionic intercalates sulfuric acid, to exfoliate graphene from pyrolytic graphite.

2. Experimental

2.1. Materials

All the chemicals and solvents used were of analytical grade and have been used without further purification. High grade pyrolytic graphite sheet of thickness 3 mm (Asbury Graphite Mills, IPG-15) was employed as both the working as well as counter electrodes in a voltage regulated DC bias system (Aplab, Model No. 7103). All experiments were conducted at ambient condition of temperature and pressure.

2.2. Electrochemical synthesis of FLGNSs

A simple aqueous protic solvent was prepared by maintaining different concentrations of $HClO_4$ (0.5, 1.0, 1.5 and 2.0 M) and doubly distilled water. A freshly cleaved graphite sheet (1.0 cm × 1.5 cm × 0.03 cm) was used as working electrode (WE) by blanketing the remaining portion by

an adhesive tape. The counter electrode was also the same type of graphite sheet used by exposing more surface area to the electrolytes. Prior to the process of exfoliation, WE was given a cathodic pre-treatment of initially at 10 V for 30 second to remove any physically adsorbed impurities and later on 3 V for 15 minute in order to make the availability of surface as well as internal lattice pores of graphite electrode for efficient intercalation. Then the pre-treated graphite electrode was connected as anode in the electrolytic bath with gradual increase of applied potential from 0 to 8 V. After ramping of applied voltage upto 8 V, the electrolytic bath has been given a constant extreme potential (i.e. 8 V) for rapid exfoliation. After that the exfoliated graphite flakes were collected from the electrolytic bath and rinsed off in double distilled water to remove any un-dissociated and ionic form of $HClO_4$ content. The dispersed product was then subjected to probe ultra-sonication for four hours to further disintegrate the graphitic flakes. The homogeneously dispersed sonicated graphene colloidal is centrifuged at 6000 rpm for 45 minute and the decant is considered as FLGNSs.

2.3. Characterization

As synthesized FLGNSs were subjected to various structural, morphological, topographical, chemical bonding and functional group analysis by high precision and calibrated scientific instruments. The X-ray diffraction (XRD) patterns of the FLGNSs powder were measured by Ultima IV system using a monochromatic Cu Kα radiation (λ = 0.154 nm) in the range of 2θ from 5-70°. Thermogravimetric analysis (TGA) of the FLGNSs were carried out by a TA Q5000IR model at a heating rate of 10°C min^{-1} under nitrogen atmosphere. Morphological analysis was carried out by a FEI Nova NanoSEM 450 Field emission scanning electron microscope (FESEM) along with Energy-dispersive x-ray spectroscopy (EDS) and by a JEM 1200 JEOL operated at 200kV Transmission electron microscope (TEM). The micro Raman spectrometer (Renishaw, UK, model Invia) with an excitation of argon ion laser of wavelength 514 nm was used at a scan range from 1000-1800 cm^{-1}. Studies on Fourier transform infrared spectroscopy (FTIR) by Shimadzu IR Prestige-21 instrument, in the range of 4000-800 cm^{-1} reveal the details about the vibrational mode of various functional groups bonded to the exfoliated FLGNSs. X-ray photoelectron spectroscopy (XPS) of AMICUS 3400, Kratos analytical Shimadzu corporation has been used for quantitative elemental analysis of the FLGNSs using Mg target under high pressure. The stability and particle size of FLGNSs colloidal samples were characterized by Malvern Zetasizer nano ZS. Furthermore the electronic transitions and band gap details form the FLGNSs colloidals were obtained from UV-visible spectroscopy in absorbance mode from 200-800 nm wavelength using Shimazdu, UV-160A model.

Furthermore, unlike above described experimental procedure, a constant applied bias of 8 V was given to the pre-treated WE in different electrolytic concentrations as mentioned above. The respective electrochemically exfoliated products were collected and analyzed initially by visual inspection and then by morphological studies. The facts of direct exfoliation at constant high applied bias were concluded and summarized in supporting information of Fig. S1 and S2, which

was found to be technically unsuitable to produce graphene nonasheets. Hence we have continued further experimentation by ramping the applied voltage (0 to 8V)and not the constant potential at 8V

3. Results and discussions

3.1. Mechanism of electrochemical intercalation and exfoliation

As mentioned in the experimental section, FLGNs has been electrochemically synthesized from pyrolytic graphite through a sequence of cathodic pretreatment at 3V trailed by anodic exfoliation through the potential range of 0 to 8 V. The pyrolytic graphite electrode used here is of synthetic grade, made by thermal graphitization of super fine graphite grains in isostatic process. These pyrolytic graphite materials consist of long range order of lamellar graphitic crystals oriented horizontally and stacked to make three-dimensional network structure. Again this graphitic crystal lamella is a layered sp^2 hybridized hexagonal carbon network weakly bonded by Van der Waals forces with the separation of 0.335 nm. Therefore, the intercalate size should be optimum enough in order to enter in between the carbon hexagonal layers. The size of the cations, anions and other gases which might get generated during the sequential cathodic and anodic process followed in the present study are mentioned Table.1.

Table 1: Sizes of different intercalate species with respect to C-C off plane distance

Element	C-C off plane distance	H^+	H_3O^+	OH^-	ClO_4^-	H_2	H_2O	CO_2	CO	O_2
Diameter (nm)	0.335	1.74×10^{-6}	0.2	0.266	0.48	0.297	0.275	0.39	0.371	0.354

The requirements of the above mentioned sequence, role of the ions/gases and the mechanism of production of FLGNs can be explained by the below mentioned points for cathodic pretreatment and anodic treatment (Figure 1):

Cathodic pretreatment:

Initially the WE is subjected to cathodic pre-treatment by applying high bias of 10 V for short period (30 second) and then 3 V for 15 minute in distilled water. At high applied potential (at 10.0 V), there is vigorous evolution of hydrogen gas at WE, resulting to remove any physiadsorbed contaminats. At later stage and during the low potential regime, slow electrolysis phenomenon to occur. As a result of this electrolysis, hydrogen ions and gas are evolved at the electrode as shown in the sequence step of Fig. 1. The H^+ ions are physically adsorbed onto graphite lattice surfaces (Equation-1) and subsequently released in the form of molecular hydrogen gas (Equation-2).

$$C_{Lattice} + H^+ \rightarrow C_{Lattice}H_{Adsorbed} \quad (1)$$

$$C_{Lattice}H_{Adsorbed} + H_2O + e^- \rightarrow C_{Lattice}(expanded) + H_2\uparrow + OH \quad (2)$$

The intensity of the intercalation mechanism either by the released ions (H^+ or H_3O^+) or cathodic gas (H_2) may not sufficient enough to generate impact between the graphite layer for exfoliation or to breakdown the Van der Waals force due to their small size as compared to the carbon layer off plane bonding distance. But the vigorous evolution of hydrogen gases at such high negative potential could be well enough to expand the inter-lamellar carbon bonding of the electrode. So this reaction step is essential to expand the graphite electrode by reducing the inter lamellar forces of attraction and make the passage available for the voluminous anionic intercalates during the anionic treatment. Furthermore it may also help to cleanse various organic and inorganic adsorbed impurities from the defect site inside the graphite crystal lattices if any.

Anodic reactions:

The cathodic pre-treated graphite electrode is then connected to anodic polarization of 0 to 8 V in aqueous $HClO_4$ electrolytes at a ramping step of 0.5 V with increase in time. As a result of linear sweep of the applied voltage, anionic species (ClO_4^- and OH^-) are intercalated the graphite lattice and as a consequences of complicated electrochemical reaction (as shown in Eqn. (3-7)) gases (O_2 and CO_2) are evolved at the working electrode. At low applied bias (0 to 5 V), initially less and finally vigorous amount of gaseous bubbles are observed at the anode (O_2 and CO_2 gas molecules) due to faradic electrochemical reactions[13]. It has been observed that the graphite electrodes were swelled during the ramping of potential at low range. This may be due to the loosening of van der Waal's like force in between the graphene basal planes. This fact is due to the release of O_2 and CO_2 gaseous species which are relatively bigger and is equal to the inter-lamellar spacing of graphite planes. Upon increasing the applied bias to 8 V, anionic species such as ClO_4^- and OH^- might have intercalated through the pyrolytic graphite sheet on the surface as well as in-depth intercalate zone of graphite lattices. Figure 1, shows the schematic flow of cathodic pretreatment, electrochemical intercalation and exfoliation process of graphite electrodes. As a result of this anionic intercalation, oxidation occurs at the anode electrode lattice sites and enriches the surface boundary of the lattice with various oxygen functional groups such as hydroxyl (-OH) and carboxylic (-COOH) groups. These intercalates reacted with graphite lattice to form graphene oxide (GO)[14,15] along other by product with release of CO_2 and O_2 gaseous molecules as shown in below reactions. Upon release of these gaseous materials from the interstitial laminar graphite planes, it further under goes surface blistering of the graphite sheet which leads to exfoliation as a few layers of graphitic flakes. Equation-7 accompanied with other electrochemical reaction (as shown in Equation- (3) to (6)), takes the major role in synthesis of few layers of graphite flakes[13].

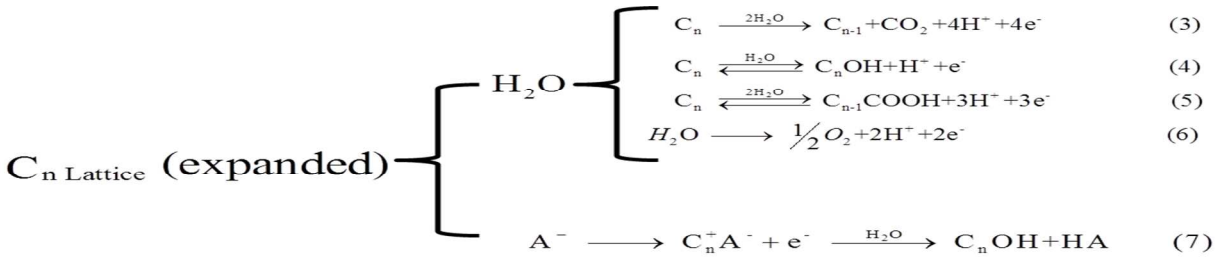

Where A stands for anions.

The exfoliated multilayered graphite flakes were collected at the bottom of the electrochemical reactor. However, light weight graphite flakes consisting of few layers of graphene nanosheets (GNSs) were found to be dispersed in the bulk electrolyte.

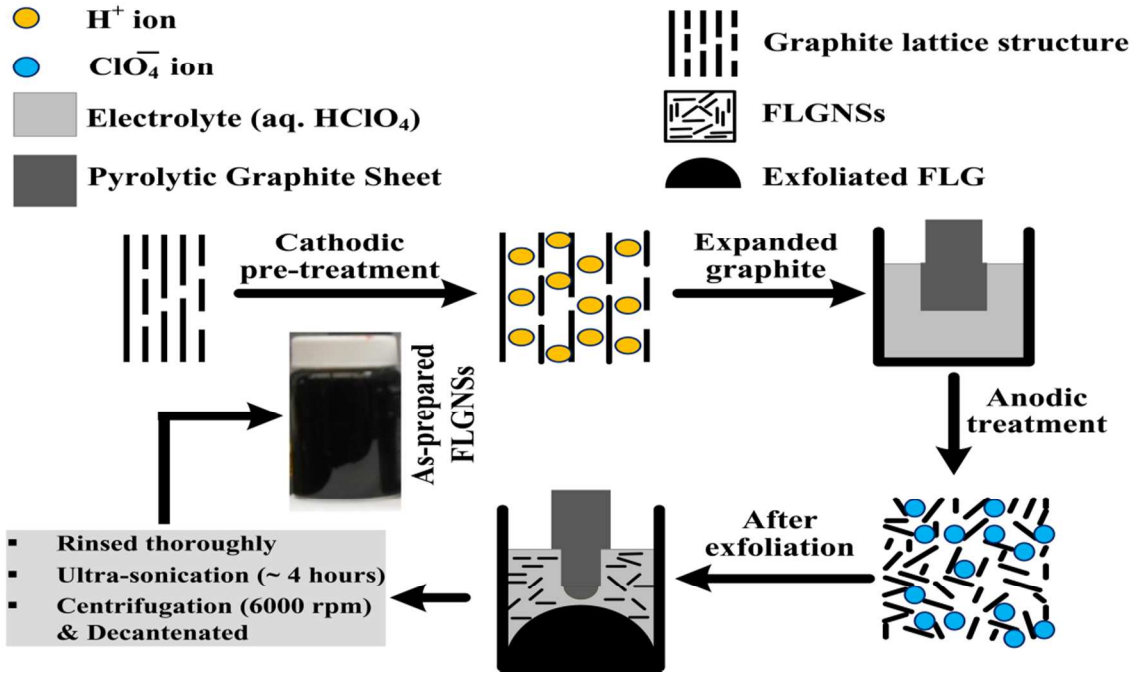

Fig. 1. Schematic flow of experimental process; electrochemical intercalation and exfoliation of pyrolytic graphite sheet for the synthesis of FLGNSs.

3.2. Linear sweep voltammetry study

Electrochemical intercalation and exfoliation process was carried out in different concentrations of electrolytes i.e. 0.5, 1.0, 1.5 and 2.0 M $HClO_4$ and are referred as PA1, PA2, PA3 and PA4 respectively. With change in applied bias to the electrode, current change at anode is noted. Figure 2 shows the relation between applied DC bias and change in current with respect to time for low and high concentration of ions. The general trend of applied voltage vs. current profile shows an initial steep increase in current, and then a decrease corresponding to the intrcalation/expansion and exfoliation respectively. At low electrolytic concentration (PA1), the

intercalation followed by exfoliation of graphitic flake is slow, which could be seen from i-v-t analysis. Accumulation of localized stress inside the graphite lattice is more prominent before exfoliations at lower intercalate concentration. Henceforth, resulting thicker graphitic flakes settling at the bottom of the electrochemical reactor. With the increase in concentration of intercalate content in the electrolytes, the process of intercalation and exfoliation produces higher average current causing peeling of very thin graphitic flakes simultaneously. The steep rise in current (up to 6.0 Amp.) indicates the fast generation of new available carbon lattices, exposed to the ionic electrolyte in the reactor chamber. After the start of full fledge exfoliation, current decreases exponentially after around 2500 second due to thinning of graphite electrodes.

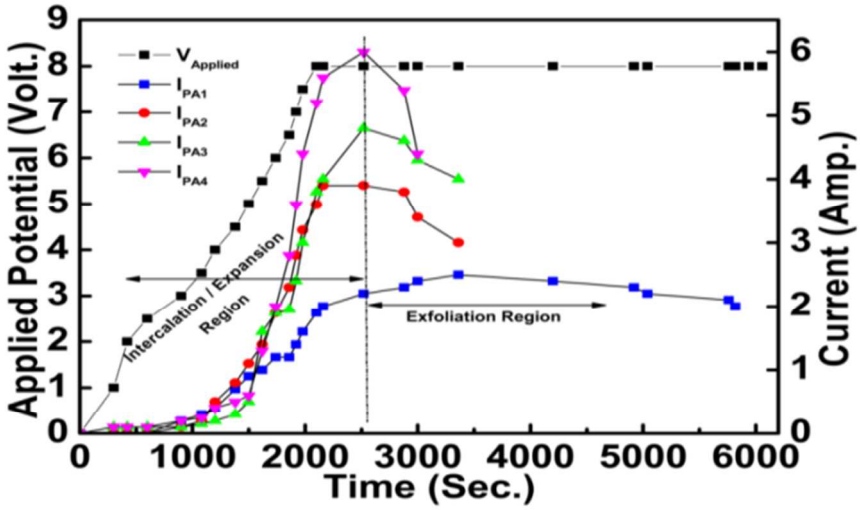

Fig. 2. Relations of Voltage-current-time during electrochemical synthesis of FLGNSs.

3.3. Stability, yield, structure and morphology of exfoliated FLGNSs

The nature and stability of electrochemically synthesized exfoliated FLGNSs colloidal at various intercalate concentration has been initially analyzed by dynamic light scattering technique. Figure 3a shows the variation of sizes of the exfoliated FLGNSs and zeta potential for the experimented four electrolyte concentrations. The average particulate size has decreased from 140 to 107 nm with the increase of electrolyte concentration due to efficient intercalation and exfoliation. Zeta potential signifies the stability of colloidal dispersions and provides a measure of the magnitude and sign of the effective surface charge associated with the double layer around the colloid particle. From a general colloidal science perspective, zeta potentials with absolute values larger than ±30 mV can result in a stable dispersion due to inter-particle electrostatic repulsion. Figure 3a shows that the zeta potential of as-synthesized FLGNSs are electrolyte concentration sensitive. The value of zeta potential increased from -25.6 mV to -37.5 mV, implying better dispersion of the FLGNSs produced at PA4. It could be due to the consequence of the negative charge on the graphene sheets that develop as a result of the ionization of the different functionalities incorporated at higher concentration of intercalates. These results are indicative of efficient electrochemical exfoliation at PA4. Again form the histogram analysis, the

uniformly dispersed graphene colloidal sheets exfoliated in PA3 and PA4 electrolytic condition shows the size distribution of 80 to 190 nm (as shown in inset of Fig. 3a). From initial visual inspection, it could be observed that the exfoliated graphitic flakes at lower perchloric electrolytic condition (i.e. 0.5 and 1.0 M) are heavier and quickly settled at the bottom of the electrolytic cell.

It would be reasonable to assume that graphene flakes exfoliated at low concentrations may consist of many layers for which it was not possible to process further to obtain FLGNs. Henceforth, further analysis have been carried for the FLGNSs exfoliated at higher intercalate concentrations of electrolytic bath conditions PA3 and PA4 (i.e. 1.5 and 2.0 M $HClO_4$). The yield of FLGNs at these two concentrations was then calculated on the basis of weight of functionalized graphene and their corresponding graphene content from TGA analysis (Fig. 3b). The detail parameters incurred for the calculation are given in Table 2. The estimated yields of the synthesized FLGNs are in the range of 40 to 44%. Though the yield is lower and well competent with the reported values[16], the current two electrode method could be potent enough for mass production of industrial grade graphene.

Table 2: Yield of FLGNSs produced at electrolytic condition of PA3 and PA4.

Electrolytic condition	Exfoliation time (in min.)	Wt. of exposed WE (in gram)	Wt. of FLGNSs (in gram)	TGA Wt. % at 500°C	Yield (%)
PA3	56	1.159	0.549	93	44
PA4	50	1.159	0.586	79	40

XRD analysis was carried out on the freshly cleaved pyrolytic graphite sheets and exfoliated FLGNSs at 1.5 and 2.0 M $HClO_4$ (Fig. 3c) electrolytic conditions in order to investigate and compare the crystallinity and d-spacing of the materials. For the pyrolytic graphite sheet, (002) plane corresponds to the basal plane of graphite hexagonal lattice, which is well observed at 2θ = 26.45° with an inter-planner spacing of 0.337 nm. In addition there are three peaks observed at 42.38°, 44.43° and 54.29° corresponding to (100), (101) and (004) crystal planes respectively (ICCD-PDF # 411487). As prepared FLGNSs from electrolytic conditions at PA3 and PA4 shows the increase of d-spacing along the (002) basal planes from 0.344 to 0.349 nm which corresponds to the peak broadening and lower angle shifting to 25.83° and 25.46°. Again the peak at 8.76° and 8.36° in case of PA3 and PA4, corresponds to partial oxygenation[17,18] of the synthesized FLGNSs. The calculated d-spacing for the above planes were around 1.009 and 1.057 nm respectively. The increase in d-spacing of FLGNSs with increase of intercalate concentration may be attributed to expansion of the stratified graphene layers with higher intercalation impact and severity of oxygenation[19,20].

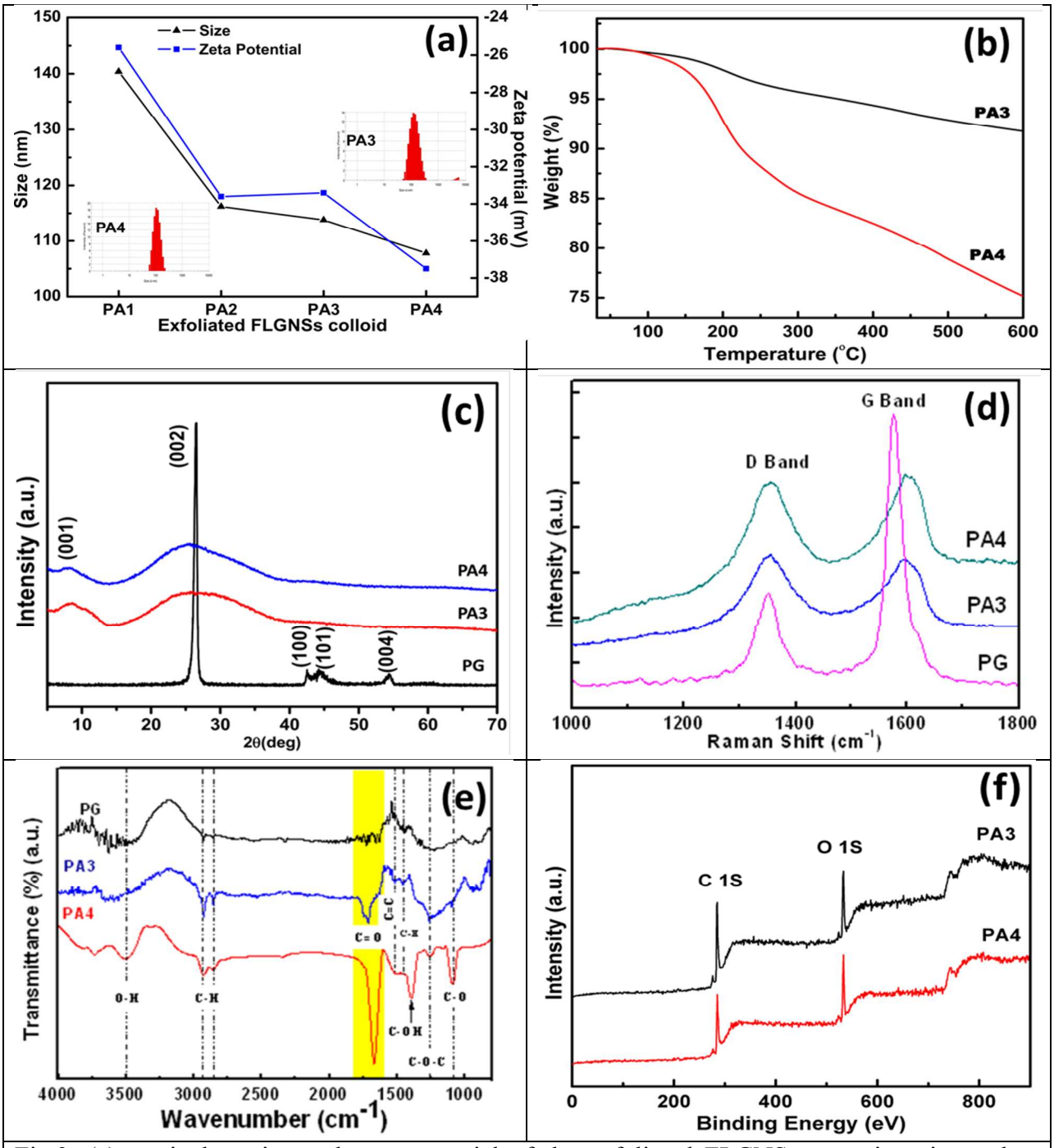

Fig.3. (a) particulate size and zeta potential of the exfoliated FLGNSs at various intercalate concentrations (inset; size distribution histogram of PA3 and PA4), (b) TGA of PA3 and PA4, (c) XRD patterns of graphite sheet and exfoliated FLGNSs, (d) Raman spectrum Pyrolytic graphite sheet and FLGNSs, (e) FTIR of the Pyrolytic graphite sheet and FLGNSs and (f) XPS of PA3 and PA4.

Raman spectroscopy is a unique and high sensitive technique used here for qualitative analyses of symmetry and disorderness of sp^2 hybridized carbon nanomaterials. The most characteristic Raman peaks at 1580 and 1350 cm^{-1} of the pyrolytic graphite as shown in Fig. 3d correspond to G and D band respectively. The G band is the signature of in-plane vibration of C-C bond form in the hexagonal carbon ring structures arising from doubly degenerate phonon mode at the Brillouin zone center[21]. The strong and intense peak of G band indicates the crystalline nature of the graphite sheets[22]. The Raman peaks from the as-prepared exfoliated FLGNSs in electrolytic conditions from PA3 and PA4 corresponding to G band are observed at 1592 and 1597 cm^{-1} respectively. Comparative low intensity and peak broadening (FWHM of 35 cm^{-1}) of the exfoliated FLGNSs could possibly be due to strain generated at the graphene sheets and reduced crystal size of sp^2-bonded carbon network i.e., nanographene. Again the upshift (~10-17 cm^{-1}) in G position of the exfoliated carbon materials may be attributed to the formation of few layer of graphene nanosheets as well as electrochemical functionalisation[23,24]. The D band in Raman spectra corresponds to the disorder or defect in the carbon hexagons structure arising from breathing mode of k-point phonons of A_{1g} symmetry owing to loss translation symmetry[22]. The peak centered at 1350 cm^{-1} in case of pyrolytic graphite is primarily due to imperfect graphite structure. After electrochemical exfoliation of the exfoliated FLGNSs, the ionic functionalization due to oxygenation and hydroxylation in the basal planes and at the edges of the carbon sheets and the reduction in graphite crystallite size might have possibly shifted and broadened (FWHM to ~ 55 cm^{-1}) D band centered at 1355 cm^{-1} for both the concentrations. Furthermore, the disorderness of the exfoliated GNSs can be quantified by the relative ratio of intensity between the D and G band (I_D/I_G)[25,26] and was found to increase form 0.39 (for pyrolytic graphite sheets) to 0.96 and 1.04 in case of PA3 and PA4 respectively. This linear increase of defect nature of the exfoliated carbon nanomaterials may primarily due to the heavy damage of carbon hexagonal ring structure during electrochemical intercalation by ClO_4^- ions into the stratified graphite electrode.

Surface oxygenation is an ineluctable phenomenon imputed with any chemical process of synthesis of the graphene nanosheets. Besides, the electrochemically exfoliated FLGNSs endowed with various oxygen functional groups with the carbon atoms that resulting from the protic solvent media with high applied potential. With increase in concentration of the electrolyte (i.e., from PA1 to PA4), the rate of oxygen endowment on FLGNSs has been found to be more prominent (please refer supplementary information Fig. S3 and Table. T1). Furthermore,The carbon structure and various functional groups attached to the electrochemically intercalated and exfoliated FLGNSs has been analyzed by FTIR spectroscopy. Fig. 3e shows FTIR spectra of the pyrolytic graphite powder, electrochemically exfoliated FLGNSs at PA3 and PA4 electrolytic conditions. The exfoliated graphene sheets show intense peaks which might correspond to the bonded functional groups as compared to the graphite spectrum. The aromatic sp^2 carbon ring, C=C stretching is well observed at around 1510 cm^{-1} [27,28]. The peak at ~ 3500 cm^{-1} corresponds to stretching vibrations of O-H functional group, which is more prominent at the higher concentration (PA4) because of larger interlayer spacing of FLGNSs. The characteristic peaks

responsible for hydroxylation arise at 2927 and 2854 cm^{-1} as well as at 1455 cm^{-1} due to C-H stretching and bending respectively[29]. The most intense peaks of oxygenation of the exfoliated FLGNSs has been observed at 1700 cm^{-1}(C=O stretching vibration; carbonyl), 1088 cm^{-1} (C-O stretching; alkoxide), 1256 cm^{-1} (C-O-C stretching; epoxide) and 1392 cm^{-1} (COO-H/CO-H stretching; carboxyl)[26–30].

To further support our claim of increase of oxidation of FLGNSs with increase in electrolyte concentration, XPS of PA3 and PA4 FLGNSs have been performed and analysed. The core levels of C1s and O1s locating at ~284.5 eV and ~532.5 eV for the electrochemically exfoliated FLGNSs in the XPS survey scan spectra as shown in Fig. 3f attribute to the presence of various oxygen functionalization in the carbon network structures[31]. The carbon, oxygen and O/C atomic ratio of PA3 and PA4 FLGNSs are calculated from the survey spectra, listed in Table 3. It has been observed that, at PA4 i.e., higher electrolytic concentration, the surface oxygenation of the FLGNSs is increased by 1.16 % than PA3. Furthermore, the detail illustration of various functional groups bonded to the FLGNSs obtained by PA3 and PA4 electrolytic exfoliation conditions are shown in Fig. S3.

Table 2: The quantitative values of Carbon (C 1s), oxygen (O 1s) element (in %) and O/C atomic ratio of PA3 and PA4 FLGNSs samples obtained by XPS survey spectra.

Sample	Elements (%)		
	C 1s	O 1s	O/C ratio
PA3	62.49	37.51	0.600
PA4	61.33	38.67	0.630

FESEM and TEM were used for morphological analysis and are shown in Fig. 4. After exfoliation, the as-prepared FLGNSs reveal a wrinkled or folded morphology with a few stacked layers (about 3–6 layers) at the edge as shown by arrow marks in PA3/TEM image. The images show partial transparency indicating the few layers of graphene sheets stacked together as well as crumpling of edges (can be depicted from arrow mark in PA4/TEM image). due to oxygenation and hydroxylation. This is originated by various defects and functional groups carrying sp^3 hybridized carbon atoms, which are introduced during the oxidation process. The semitransparent/transparent-looking GO flakes are found to be similar to those synthesized by other researchers using chemical and electrochemical processes. In general, graphene oxide nanosheets tend to assemble with each other and forms multilayer agglomerate.

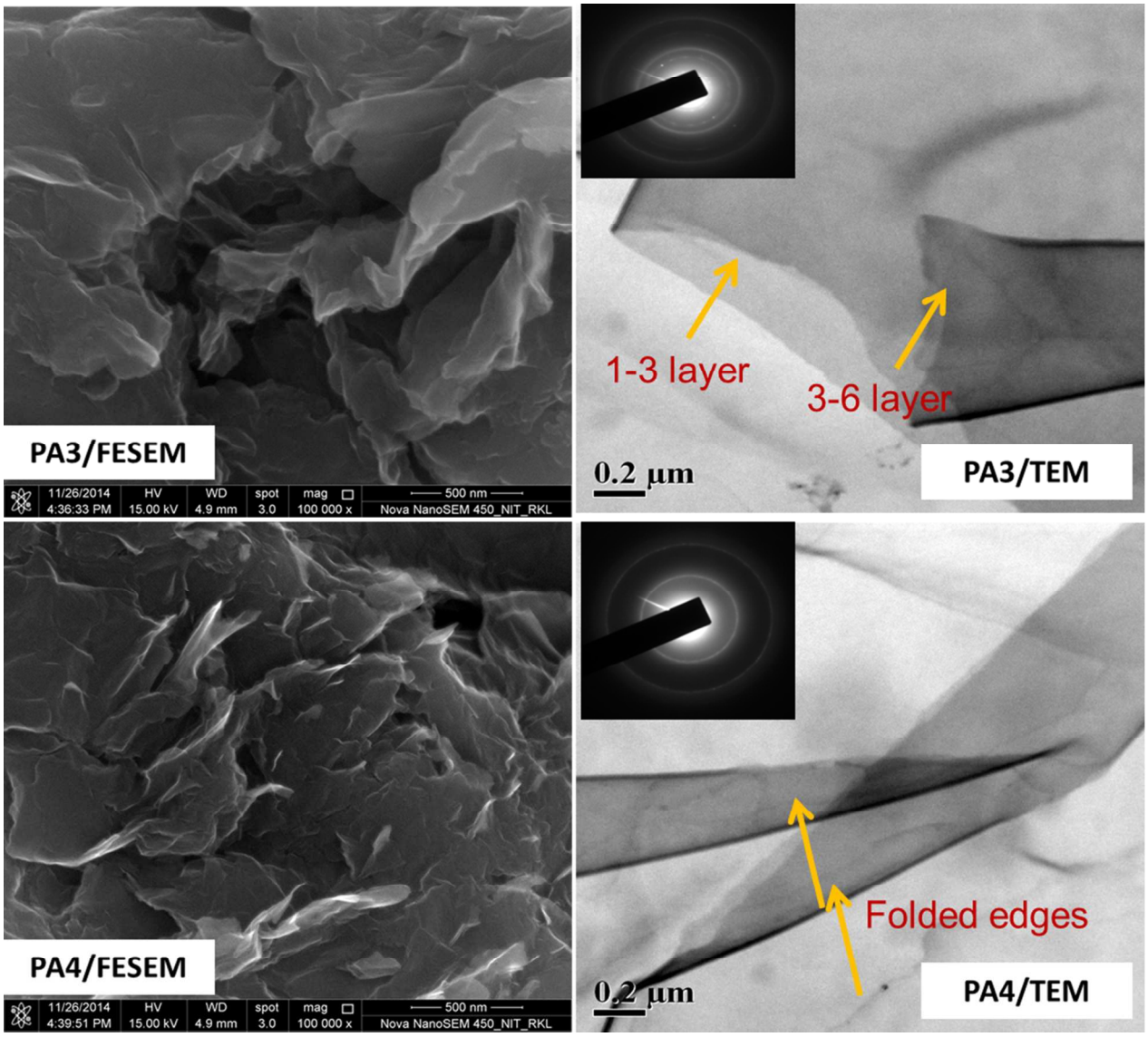

Fig.4. FESEM and TEM (inset; SAED pattern) images of FLGNSs obtained at PA3 and PA4 electrolytic condition.

However, in TEM image, the presence of topological features along with overlapping area of graphene oxide nanosheets reveals that they are highly dispersed in water. The crystallographic structure of the graphene sheets was characterized by SAED (inset) pattern. Generally graphene sheets exhibit a single set of hexagonal diffraction pattern with sharp and clear diffraction spots[32]. In the present study the patterns reveal the presence of bright diffraction spots along with ring pattern for FLGNS at PA3, whereas the rings are sharp for graphene nano-sheets synthesized at PA4. This can confirm the fact that the as synthesized PA4 FLGNSs have partial crystallinity[33] as compared to those observed in case of PA3 exfoliated FGNSs. This may be because of increase of order of amorphocity due to crawling of edges and surface functionalization in the FLGNSs from PA3 to PA4.

3.4 Optical and electrical conductivity studies

The UV-visible spectrum of anodically exfoliated FLGNSs (as shown in Fig. 5a) from an acidic bath at different concentration show broad peak around 260 nm, which is primarily observed due to π-π* electronic transitions of carbon-carbon (C-C) aromatic ring in graphene sheets. A small shoulder at around at 300 nm is also seen for both the concentrations. This absorption of the visible light is mainly due to the n-π* transitions of carbonyl group (C=O)[28,34]. The optical band gaps of the FLGNSs were determined by using Tauc plot through an extrapolation of the linear region in the UV spectra (inset Figure). Due to non-uniform oxygen functionalization in FLGNSs, a smooth adsorption edges has been observed in the Tauc plot. From calculation, the electrochemically exfoliated graphene colloidal exhibits an approximate band gap ranges over 2.11 - 2.96 and 2.73 - 3.35 eV for PA3 and PA4 electrolytic conditions respectively. Furthermore the transmittance of the electrochemically exfoliated FLGNSs at 550 nm are 84.5 and 92.7 for PA3 and PA4 respectively. Considering graphene single layer absorbance of 2.3 % in white light, it can be estimated that the as-prepared FLGNSs consist of layers of around 6 and 3 for PA3 and PA4 respectively. Thus increase in band gap with decrease in number of layers may be assigned for heavy insertion of perchlorate ions (ClO_4^-) and increase in space in between layers of FLGNSs exfoliated at higher acid concentration.

Exfolaited FLGNSs colloidal conductivity analyses were carried out by an indigenous setup and the extrapolate is shown in Fig. 5b. The aqueous dispersed graphene colloidal exfoliated at different electrolytic concentration (e.g. PA1, PA2, PA3 and PA4) were used as electrolyte and two copper foils with surface area of 1.44 cm^2 served as electrodes for the electrical measurements. A DC supply of up to 0.6 V, well below the electrolysis of water is then applied to the copper sheets by Keithley-2400 source meter.

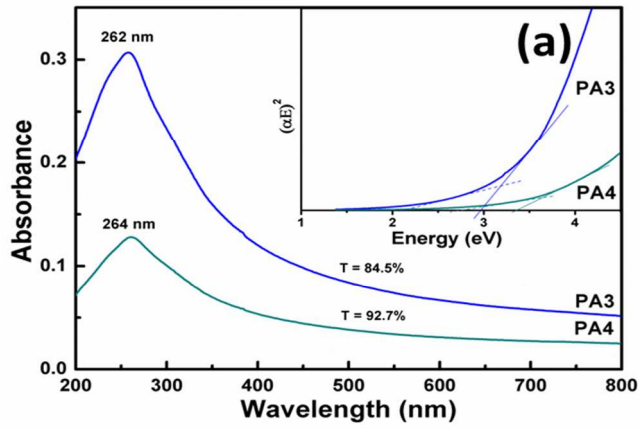

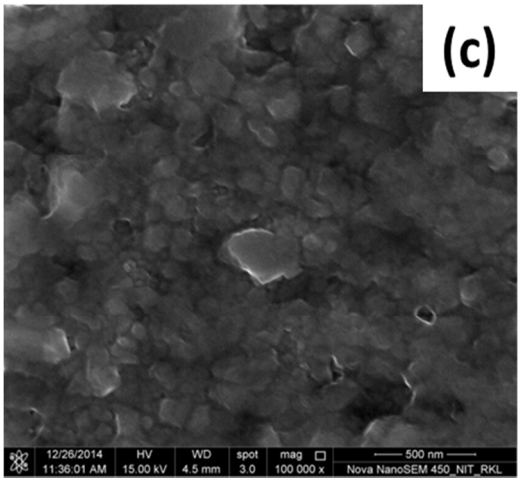

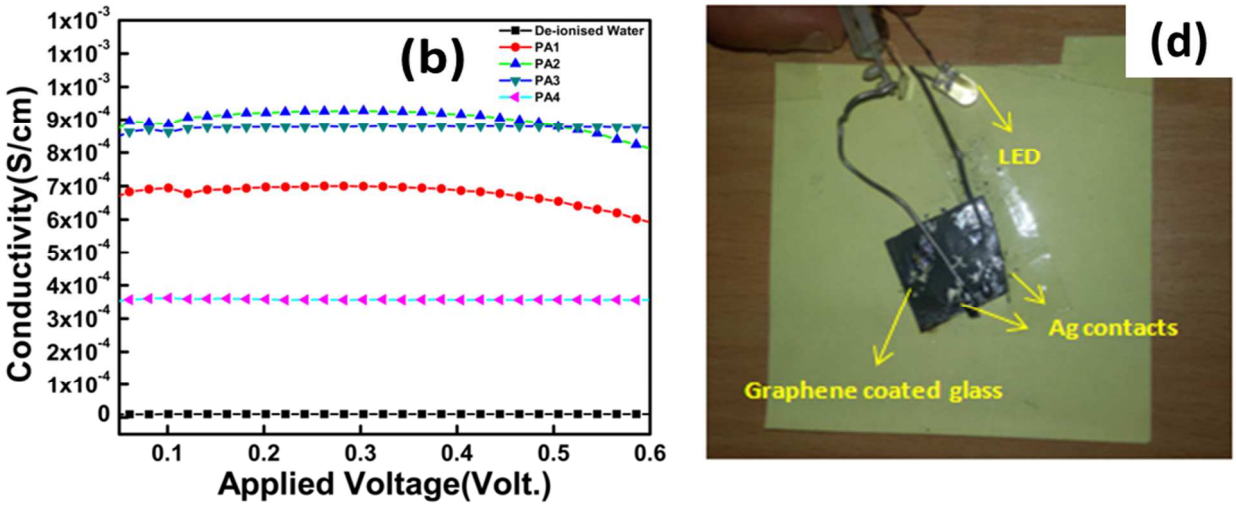

Fig. 5. (a) UV-visible spectra of electrochemical exfoliated FLGNSs, (b) electrical conductivity of FLGNSs, (c) FESEM micrograph of graphene coated glass and (d) LED test on graphene coated glass substrate.

From Fig. 5b, it can be seen that de-ionised water has the lowest conductivity (~9.89 µS/cm) which confirms the absence of any free ions for the conduction. Upon dispersion of as-prepared GNSs, the conductivity was increased from 0.67, 0.892, 0.87 to 0.35 mS/cm for PA1, PA2, PA3 and PA4 respectively. The low value at PA1 may attribute to lack of continuity or homogeneous distribution of heavy graphitic flake, which was observed to easily settle down at the bottom of test reactor. At PA2, the conductivity rises significantly to 0.892 mS/cm due to lower oxidation and homogeneous distribution of FLGNSs but the comparative heavy flake destabilize to retain its conductivity with increase of applied bias. However, FLGNSs prepared at PA3 make a stable dispersed graphene colloidal of stable conductivity 0.87 mS/cm. Though the FLGNSs at PA4 are stable and homogeneously dispersed, the conductivity was found to get decreased to 0.356 mS/cm. This observation may be due to presence of functional groups because of heavy oxygenation of GNSs during intercalation and exfoliation.

The FLGNs obtained at PA3 was used to coat a glass substrate and further test the conducting property. A conformal coating of the conductive ink has been fabricated in a Hydrogen fluoride (HF) etched glass slide and was then oven dried. Fig. 5c shows the FESEM micrograph of the coated graphene substrate. It can be observed that the coating is uniform and adherent to the glass. Furthermore a LED test has been carried out to compile the conductive nature of the PA3 FLGNSs colloids. The LED contacts were made through silver paste on the coated glass substrate. A series connected 4.5 V cell type battery was connected to the LED through the silver plated electrode. Prior to the applied voltage, zero continuity of the plated electrode was confirmed through a multimeter. At the applied voltage, the glowing of the LED (Fig. 5d) confirms the high conductive nature of the as-synthesized FLGNSs at PA3 electrolytic condition. The same LED test has also been carried out after a month, an unchanged behavior was noticed.

4. Conclusion

An efficient and scaled anionic intercalation and exfoliation process for synthesis of FLGNSs from the pyrolytic graphite sheets has been conducted in the present report. The anionic intrecalate used here was perchlorate ions (ClO_4^-) with varying concentrations of 0.5, 1, 1.5 and 2 M. Intercalate concentration of the protic solvent plays prominent role for quality synthesis of the graphene nanosheets by the electrochemical technique. From particle size and zeta potential measurements, the FLGNSs colloids show very stable dispersion at high intercalate concentrations with decrease in size of the graphene sheets. It was also observed that the defects and amorphous nature in the exfoliated sheets increases along with increase in intercalate concentration which has been confirmed by morphological and Raman studies. XRD, FT-IR and UV-visible spectroscopy analysis shows the partial oxygenation of the exfoliated FLGNSs along with π-conjugation aromatic ring structured graphene basal planes. The reported analyses may pave way for a synthesis route for industrial level of production of thin layered and higher domains of graphene sheets which could be coated as thin films with high specific surface area. However the study needs further critical experimentations before drawing an articulate conclusion.

Acknowledgement

The authors would like to acknowledge the financial and infrastructure support received from National Institute of Technology, Rourkela, India.

References

1 M. Noel and R. Santhanam, *J. Power Sources*, 1998, **72**, 53–65.

2 G.-C. Chung, H.-J. Kim, S.-I. Yu, S.-H. Jun, J. Choi and M.-H. Kim, *J. Electrochem. Soc.*, 2000, **147**, 4391–4398.

3 H. Huang, Y. Xia, X. Tao, J. Du, J. Fang, Y. Gan and W. Zhang, *J. Mater. Chem.*, 2012, **22**, 10452.

4 A. J. Cooper, N. R. Wilson, I. A. Kinloch and R. A. W. Dryfe, *Carbon N. Y.*, 2013, **66**, 340–350.

5 J. Wang, K. K. Manga, Q. Bao and K. P. Loh, *J. Am. Chem. Soc.*, 2011, **133**, 8888–8891.

6 Y. Yang, F. Lu, Z. Zhou, W. Song, Q. Chen and X. Ji, *Electrochim. Acta*, 2013, **113**, 9–16.

7 C. Y. Su, A. Y. Lu, Y. Xu, F. R. Chen, A. N. Khlobystov and L. J. Li, *ACS Nano*, 2011, **5**, 2332–2339.

8 G. M. Morales, P. Schifani, G. Ellis, C. Ballesteros, G. Martínez, C. Barbero and H. J. Salavagione, *Carbon N. Y.*, 2011, **49**, 2809–2816.

9 D. W. Skaf and E. J.K., *Synth. Met.*, 1992, **46**, 137–145.

10 G. Wang, B. Wang, J. Park, Y. Wang, B. Sun and J. Yao, *Carbon N. Y.*, 2009, **47**, 3242–3246.

11 M. Hofmann, W.-Y. Chiang, T. D Nguyn and Y.-P. Hsieh, *Nanotechnology*, 2015, **26**, 335607.

12 S. K. Sahoo and A. Mallik, *Nano*, 2015, **10**, 1550019.

13 J. Liu, C. K. Poh, D. Zhan, L. Lai, S. H. Lim, L. Wang, X. Liu, N. Gopal Sahoo, C. Li, Z. Shen and J. Lin, *Nano Energy*, 2013, **2**, 377–386.

14 A. a Gewirth and A. J. Bard, *J. Phys. Chem.*, 1988, **92**, 5563–5566.

15 K. W. Hathcock, J. C. Brumfield, C. A. Goss, E. A. Irene and R. W. Murray, *Anal. Chem.*, 1995, **67**, 2201–2206.

16 Y. L. Zhong and T. M. Swager, *J. Am. Chem. Soc.*, 2012, **134**, 17896–17899.

17 R. Xie, G. Fan, Q. Ma, L. Yang and F. Li, *J. Mater. Chem. A*, 2014, **2**, 7880.

18 S. Bose, T. Kuila, A. K. Mishra, N. H. Kim and J. H. Lee, *J. Mater. Chem.*, 2012, **22**, 9696.

19 K. Zhang, Y. Zhang and S. Wang, *Sci. Rep.*, 2013, **3**, 3448.

20 M. Fang, K. Wang, H. Lu, Y. Yang and S. Nutt, *J. Mater. Chem.*, 2009, **19**, 7098.

21 J. Lu, J. xiang Yang, J. Wang, A. Lim, S. Wang and K. P. Loh, *Acsnano*, 2009, **3**, 2367–2375.

22 M. S. Dresselhaus, A. Jorio, A. G. Souza Filho and R. Saito, *Philos. Trans. R. Soc. A*, 2010, **368**, 5355–77.

23 M. W. Iqbal, A. K. Singh, M. Z. Iqbal and J. Eom, *J. physics. Condens. matter*, 2012, **24**, 335301.

24 A. C. Ferrari, J. C. Meyer, V. Scardaci, C. Casiraghi, M. Lazzeri, F. Mauri, S. Piscanec, D. Jiang, K. S. Novoselov, S. Roth and A. K. Geim, *Phys. Rev. Lett.*, 2006, **97**, 1–4.

25 A. Jorio, *ISRN Nanotechnol.*, 2012, **2012**, 1–16.

26 Z. Tang, L. Zhang, C. Zeng, T. Lin and B. Guo, *Soft Matter*, 2012, **8**, 9214–9220.

27 N. A. Kumar, H. Choi, Y. R. Shin, D. W. Chang and L. Dai, *ACS Nano*, 2012, **6**, 1715–1723.

28 Y. Fu, J. Zhang, H. Liu, W. C. Hiscox and Y. Gu, *J. Mater. Chem. A*, 2013, **1**, 2663–2674.

29 A. Kaniyoor, R. I. Jafri, T. Arockiadoss and S. Ramaprabhu, *Nanoscale*, 2009, **1**, 382–386.

30 M. Naebe, J. Wang, A. Amini, H. Khayyam, N. Hameed, L. H. Li, Y. Chen and B. Fox, *Sci. Rep.*, 2014, **4**, 4375.

31 W. Song, X. Ji, W. Deng, Q. Chen, C. Shen and C. E. Banks, *Phys. Chem. Chem. Phys.*, 2013, **15**, 4799–4803.

32 C.-T. Pan, J. a. Hinks, Q. M. Ramasse, G. Greaves, U. Bangert, S. E. Donnelly and S. J. Haigh, *Sci. Rep.*, 2014, **4**, 6334.

33 J. Yang, J. Chen, S. Yu, X. Yan and Q. Xue, *Carbon N. Y.*, 2010, **48**, 2665–2668.

34 J. Shang, L. Ma, J. Li, W. Ai, T. Yu and G. G. Gurzadyan, *Sci. Rep.*, 2012, **2**, 792.

Graphical Abstract:

Few-layered conductive graphene nanosheets have been synthesized by a protic intercalate electrolyte in a two electrode electrochemical intercalation and exfoliation process.